Structured triglyceride attenuates lung injury and inflammation in lipopolysaccharide-induced acute lung injury by enhancing GPR120 expression

HAIYUN SUN, YANMIN PANG, DAN ZHAO and WENYAO LI

Department of Intensive Care Unit, Heze Municipal Hospital, Heze, Shandong 274031, P.R. China

Received August 29, 2020; Accepted February 5, 2021

DOI: 10.3892/mmr.2021.12098

Abstract. Acute lung injury (ALI) is a serious clinical problem. The present study was performed to investigate the effect of structured triglyceride (STG) on the development of lipopolysaccharide (LPS)-induced ALI and its underlying mechanism of action. To establish an LPS-induced ALI mouse model, mice were intranasally administered 50 μl LPS. The pathological changes in the lung were observed via haematoxylin-eosin staining. The lung injury score, lung wet/dry weight (W/D) ratio, and myeloperoxidase (MPO) activity were used to evaluate the degree of lung injury. The expression levels of interleukin (IL)-1β, IL-6 and tumour necrosis factor-α in lung tissues were measured through reverse transcription-quantitative polymerase chain reaction. The enzyme-linked immunosorbent assay was used to measure the levels of pro-inflammatory cytokines in bronchoalveolar lavage fluid. Furthermore, western blotting was performed to detect the activity of the transforming growth factor-α-activated kinase 1 (TAK1)/NF-κB pathway. LPS-induced ALI mice were treated with AH7614 [a G-protein coupled receptor 120 (GPR120) inhibitor] to confirm the effect of STG on GPR120. STG treatment decreased the lung pathological changes, lung injury score, lung W/D ratio, and proinflammatory cytokine expression levels and inhibited TAK1/NF-κB pathway activity in the LPS-induced ALI mouse model. Additionally, AH7614 reversed the inhibitory effects of STG on lung injury, inflammation, and TAK1/NF-κB pathway activity in ALI. Moreover, AH7614 weakened the inhibitory effects of STG on inflammation and TAK1/NF-κB pathway activity in LPS-induced RAW264.7 cells. Collectively, STG may suppress the TAK1/NF-κB pathway activity by enhancing GPR120 expression to alleviate the lung injury and inflammation in ALI. These results suggest the therapeutic potential of STG in the treatment of ALI.

Correspondence to: Dr Wenyao Li, Department of Intensive Care Unit, Heze Municipal Hospital, 2888 Caozhou Road, Mudan, Heze, Shandong 274031, P.R. China
E-mail: liwenyao290@163.com

Key words: structured triglyceride, acute lung injury, G-protein coupled receptor 120, transforming growth factor-α-activated kinase 1, inflammation

Introduction

Acute lung injury (ALI) is a serious pathological condition characterised by neutrophil-derived inflammation, surfactant dysfunction, diffuse alveolar injury and lung oedema formation (1). Clinically, ALI is characterised by bilateral pulmonary infiltrates, decreased lung compliance and severe hypoxemia (2). ALI is a common, costly, and potentially lethal disease (3). It is estimated that ALI accounts for ~79,000 deaths per year in the United States, and was one of the top 8 causes of death in 2018 (4). Despite extensive large-scale clinical studies and trials, no effective treatments for ALI have been identified (5). Thus, it is essential to investigate novel approaches for the treatment of ALI.

Fat emulsions are typically regarded as a caloric source that is required to alleviate essential fatty acid (FA) deficiency in critically ill patients, including those with ALI (6). Certain fat emulsions attenuate injury and inflammation in different organs. For instance, fish oil-based fat emulsion suppresses injury and inflammation in mice with acute kidney injury (7). Fish oil-based fat emulsion decreases lipopolysaccharide (LPS)-induced alveolar leukocyte transmigration and pro-inflammatory cytokine expression in ALI mice (8). However, certain fat emulsions may induce side effects in patients with lung injury due to the presence of medium-chain triacylglycerols (MCTs) (9,10). To improve the tolerance and effectiveness of fat emulsions, a structured triglyceride (STG), which is a combination of MCTs and long-chain triglycerides (LCTs) and is also known as a structured fat emulsion or structured lipid, has been proposed (11). Treatment with STG ameliorates the inflammation in rats undergoing a total gastrectomy (12). Furthermore, STG alleviates renal injury in diabetic rats (13). However, the specific regulatory role of STG in ALI remains unclear.

G protein-coupled receptors (GPRs), including GPR120, are pivotal signalling molecules in multiple aspects of cellular function (14). GPR120 exerts anti-inflammatory effects in various diseases. Activation of GPR120 protects against focal cerebral ischaemic injury in mice by attenuating apoptosis and inflammation (15). Flaxseed oil has been found to increase GPR120 expression, thereby restraining

the inflammatory response in the livers of obese mice (16). STG represents an innovative way to supply a mixture of FAs with different chain lengths (17). GPR120 serves as an omega-3 (ω-3) FA receptor that exerts anti-inflammatory effects (18). Ginsenoside Rb2 promotes the anti-inflammatory effects of ω-3 FA in LPS-induced RAW264.7 macrophages by enhancing GPR120 (19). However, whether the effects of STG are mediated via GPR120 in ALI remains unknown.

An LPS-induced ALI mouse model was constructed in the present study and the regulatory effects of STG on lung injury, lung inflammation, and transforming growth factor-α-activated kinase 1 (TAK1)/NF-κB pathway activity in ALI was evaluated. Moreover, the associations between STG and GPR120 were identified. Thus, the present study suggests a potential compound for treating ALI.

Materials and methods

Animals and drugs. In total, 40 male C57BL/6 mice (age, 8 weeks; body weight, 22-26 g) were purchased from Beijing Vital River Laboratory Animal Technology Co., Ltd. Mice were fed standard chow and water and maintained at 22-25˚C and 55-65% relative humidity with a 12-h light/dark cycle. The animal experiments were approved by the Ethics Committee of Heze Municipal Hospital (approval no. KYLL-hzsl2020008). STG is an innovative mixture of MCTs and LCTs containing combinations different from chain length FAs. The STG used in the present study was purchased from FRESENIUS (C_{6-24}).

ALI mouse model. After 1 week of adjustment, 20 mice were randomly allocated into four groups (n=5): Sham, ALI, ALI + STG 2.5 mg/kg and ALI + STG 7.5 mg/kg. To establish the LPS-induced ALI mouse model, mice were intranasally administered 50 μl LPS. The Sham group was intranasally administered 50 μl PBS. Then, 1 day postperfusion, mice in the ALI + STG 2.5 mg/kg and ALI + STG 7.5 mg/kg groups were intravenously injected via the tail with 2.5 or 7.5 mg/kg STG three times at 6, 12 and 18 h. Mice in the ALI group received only LPS administration. Moreover, 20 additional mice were randomly divided into four groups (n=5): Sham, ALI, ALI + STG and ALI + STG + AH7614. The protocol of the Sham, ALI and ALI + STG groups was consistent with the previously described Sham, ALI and ALI + STG 7.5 mg/kg groups, respectively. Additionally, AH7614 (GPR120 inhibitor) was used to further investigate the association between STG and the GPR120. In the ALI + STG + AH7614 group, LPS-induced ALI mice were intravenously injected via the tail with 7.5 mg/kg STG three times at 6, 12 and 18 h prior to receiving 50 μg/mg AH7614 by intravenous tail injection.

Sample collection. A total of 1 h after the last treatment, all mice were anaesthetised by intraperitoneal injection of sodium pentobarbital (50 mg/kg). Blood was extracted through the hepatic portal vein under aseptic conditions and centrifuged at 3,000 x g for 15 min at 4˚C. Both the STG-containing serum and other serum were filtered through a 0.22-μm filter membrane and stored at -80˚C for cell culture. Then, 1 day later, all mice were anaesthetised and sacrificed by decapitation. Bronchoalveolar lavage fluid (BALF) was acquired by lavaging the left lung with 4 ml PBS through the tracheal cannula. The left lung was collected for measurement of the lung wet/dry weight (W/D) ratio assay. The right lung was separated, and a part of the lung tissue was fixed (24 h, 37˚C) in 4% paraformaldehyde for haematoxylin and eosin (H&E) staining (0.5% hematoxylin for 2 min at 37˚C, followed by 0.5% eosin for 2 min at 37˚C). Another part of the right lung tissue was stored at -80˚C for reverse transcription-quantitative PCR (RT-qPCR), western blotting and measurement of myeloperoxidase (MPO) activity.

Analysis of lung W/D ratio. The left lung was carefully rinsed, blotted and weighed (wet weight). Subsequently, the left lung was dried in an oven for 24 h at 80˚C and weighed (dry weight). The lung W/D ratio was calculated as follows: (Wet weight/dry weight) x100%.

MPO activity. The lung homogenates were centrifuged at 1,000 x g for 10 min at 4˚C. The MPO in the supernatant was assayed using commercial kits (Nanjing Jiancheng Bioengineering Institute).

H&E staining. Lung tissues were fixed in 4% paraformaldehyde for 24 h at 37˚C, embedded in paraffin, cut into 5-μm-thick sections and stained with 0.5% hematoxylin for 2 min at 37˚C, followed by 0.5% eosin for 2 min at 37˚C. By means of light microscopy (magnification, x400; BX51; Olympus Corporation), the lung pathological changes were evaluated. Lung injury was scored using a 5-point system according to a previous study (20). The scoring criteria were as follows: 0, normal tissue; 1, tiny inflammatory change; 2, mild to moderate inflammatory change (no marked damage to the lung architecture); 3, moderate inflammatory injury (thickening of the alveolar septa); 4, moderate to severe inflammatory injury (formation of nodules or areas of pneumonitis); and 5, severe inflammatory injury (total obliteration of the field).

ELISA. BALF was collected. After being centrifuged at 3,000 x g for 10 min at 4˚C, the supernatant was collected for cytokine detection. The levels of interleukin (IL)-1β, IL-6 and tumour necrosis factor-α (TNF-α) in BALF were assessed using mouse IL-1β ELISA kit (cat. no. RAB0275MSDS; Sigma-Aldrich; Merck KGaA), mouse IL-6 ELISA kit (cat. no. RAB0309MSDS; Sigma-Aldrich; Merck KGaA), and mouse TNF-α ELISA kit (cat. no. RAB0477MSDS; Sigma-Aldrich; Merck KGaA), respectively.

Cell culture and treatment. RAW264.7 cells (murine macrophage cell line) were cultured in DMEM/F12 medium (American Type Culture Collection) with 10% FBS (Invitrogen; Thermo Fisher Scientific, Inc.) at 37˚C and in 5% CO_2. RAW264.7 cells were divided into the negative control (RAW264.7 cells pre-treated with serum from mice in the Sham group for 1 h at 37˚C), LPS (RAW264.7 cells pre-treated with serum from mice in the ALI group for 1 h and then stimulated with 0.5 μg/ml LPS for 6 h at 37˚C), and LPS + STG serum (RAW264.7 cells pre-treated with serum from mice in the ALI + STG group for 1 h and then stimulated with 0.5 μg/ml LPS for 6 h at 37˚C) groups. Additionally, the LPS + STG serum + AH7614 group comprised RAW264.7 cells pre-treated with serum from mice in the ALI + STG +

AH7614 group for 1 h, stimulated with 0.5 μg/ml LPS for 6 h, and treated with 100 μM AH7614 for another 4 h at 37˚C.

RT-qPCR. Total RNA was extracted from tissues and cells using TRIzol® reagent (Invitrogen; Thermo Fisher Scientific, Inc.). Thereafter, complementary DNA samples were attained through RT using PrimeScript RT Reagent kit (Takara Bio, Inc.). The reaction mixtures were incubated at 37˚C for 60 min, 95˚C for 5 min and then held at 4˚C. RT-qPCR analysis was detected using SYBR-Green PCR Master Mix (Takara Bio, Inc.). RT-qPCR was conducted on the 7500 Real-Time PCR system (Applied Biosystems; Thermo Fisher Scientific, Inc.), and the reaction conditions were as follows: Initial denaturation at 95˚C for 10 min, followed by 40 cycles at 95˚C for 10 sec, 60˚C for 20 sec and 72˚C for 34 sec. The relative protein expression level was calculated using the $2^{-\Delta\Delta Cq}$ method (21). The primer sequences used are shown in Table I.

Table I. Primer sequences used in reverse transcription-quantitative PCR.

Name of primer	Sequence 5'-3'
IL-1β-F	GGTCAAAGGTTTGGAAGCAG
IL-1β-R	TGTGAAATGCCACCTTTTGA
IL-6-F	TAGTCCTTCCTACCCCAATTTCC
IL-6-R	TTGGTCCTTAGCCACTCCTTC
TNF-α-F	ATGGGAAGGGAATGAATCCACC
TNF-α-R	GTCCACATCCTGTAGGGCGTCT
β-actin-F	GGGAAATCGTGCGTGACATTAAG
β-actin-R	TGTGTTGGCGTACAGGTCTTTG

F, forward; R, reverse; IL, interleukin; TNF-α, tumor necrosis factor-α.

Western blotting. Total proteins were extracted from tissues and cells using RIPA lysis buffer (Beyotime Institute of Biotechnology). The concentration of total protein was detected using the bicinchoninic acid method. The proteins (20 μg per lane) were then separated by 10-12% sodium dodecyl sulphate gel electrophoresis gels. Separated protein was transferred onto polyvinylidene fluoride membranes, blocked with 5% skim milk for 1 h at 37˚C, and incubated at 4˚C overnight with primary antibodies, including anti-GPR120 (1:1,000; cat. no. SAB4501490MSDS; Sigma-Aldrich; Merck KGaA), anti-p65 (1:1,000; cat. no. SAB4301496MSDS; Sigma-Aldrich; Merck KGaA), anti-phosphorylated (p)-p65 (1:500; cat. no. MAB3026MSDS; Sigma-Aldrich; Merck KGaA), anti-TAK1 (1:1,000, cat. no. SAB4502922MSDS; Sigma-Aldrich; Merck KGaA), anti-p-TAK1 (1:500; cat. no WH0006885M2MSDS; Sigma-Aldrich; Merck KGaA), anti-Toll-like receptor 4 (TLR4; 1:500; cat. no. PRS3141MSDS; Sigma-Aldrich; Merck KGaA), and anti-family pyrin domain-containing 3 (NLRP3; 1:500; cat. no. HPA012878MSDS; Sigma-Aldrich) antibodies. Thereafter, the membranes were subjected to the horseradish peroxidase-labelled goat anti-rabbit IgG (1:5,000; cat. no. 12-348MSDS; Sigma-Aldrich; Merck KGaA) secondary antibody at 25˚C for 1 h. The immunoblots were analysed via enhanced chemiluminescence (Invitrogen; Thermo Fisher Scientific, Inc.) and semi-quantified using the ImageLab software (version 3.0; Bio-Rad Laboratories, Inc.).

Statistical analysis. Statistical analysis of the data was performed using GraphPad Prism 7.0 (GraphPad Software, Inc.). Data are presented as the mean ± standard deviation. The differences among multiple groups were assessed using one-way ANOVA followed by Tukey's post-hoc test. *In vivo*, the experiments were repeated three times for each mouse. *In vitro*, the experiments were performed in triplicate and repeated three times. P<0.05 was considered to indicate statistically significant differences.

Results

STG alleviates lung injury in the LPS-induced ALI mouse model. To investigate the roles of STG in the pathogenesis of ALI, an LPS-induced ALI mouse model was established. LPS administration caused considerable neutrophil infiltration, haemorrhage, interstitial oedema and thickening of the alveolar septum. Treatment with STG markedly alleviated pathological changes at both concentrations, although 7.5 mg/kg STG displayed more favourable results (Fig. 1A). Furthermore, the lung injury score was clearly elevated by LPS administration (P<0.001). Low STG concentration markedly decreased the lung injury score (P<0.01), and a high concentration of STG exhibited a more favourable result (P<0.001; Fig. 1B). Following LPS administration, the lung W/D ratio was markedly increased (P<0.001). The LPS-induced ALI mouse model treated with STG exhibited a dose-dependent reduction in the lung W/D ratio (P<0.001; Fig. 1C). Determination of MPO activity was used to assess lung neutrophil infiltration. As depicted in Fig. 1D, MPO activity was elevated in ALI lung tissues (P<0.001). STG decreased lung MPO activity in a concentration-dependent manner (P<0.001).

STG attenuates lung inflammation in the LPS-induced ALI mouse model. Inflammation was evaluated by examining the pro-inflammatory cytokine expression levels in lung tissues and BALF. As illustrated in Fig. 2A and B, the expression levels of IL-1β, IL-6 and TNF-α in lung tissues and BALF were significantly elevated following LPS administration (P<0.001). The LPS-induced ALI mouse model treated with STG displayed a dose-dependent reduction in the expression levels of IL-1β, IL-6 and TNF-α (P<0.001). Moreover, GPR120 protein expression was clearly inhibited in the LPS-induced ALI mouse model (P<0.001). STG markedly enhanced GPR120 protein expression (P<0.001). Notably, AH7614 clearly weakened the promotive effect of STG on GPR120 protein expression (P<0.001; Fig. 2C). As displayed in Fig. 2D, GPR120 expression in the ALI group was lower compared with that in the sham group (P<0.001). STG increased GPR120 expression in ALI mice (P<0.001), while AH7614 markedly reversed the promotive effect of STG on GPR120 expression (P<0.001).

STG alleviates lung injury in the LPS-induced ALI mouse model by enhancing GPR120. AH7614 was intravenously

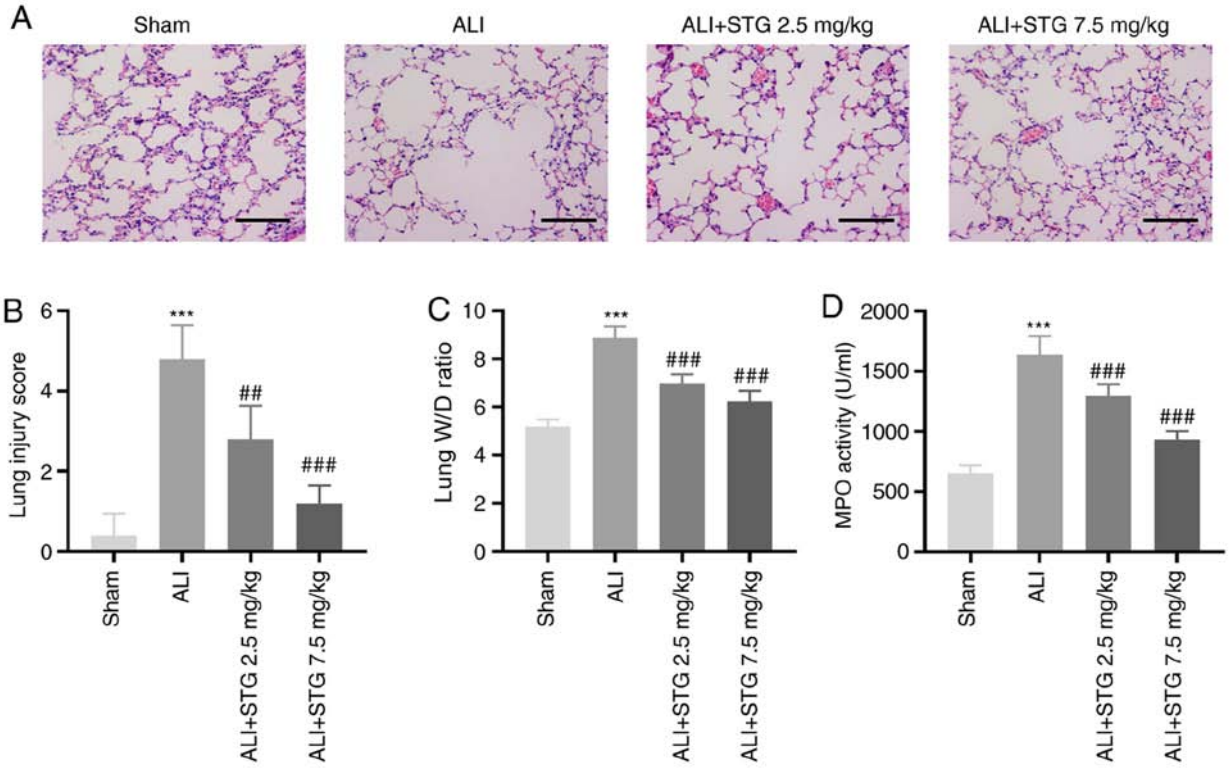

Figure 1. STG alleviates lung injury in the LPS-induced ALI mouse model. (A) The lung pathological changes, such as neutrophil infiltration, haemorrhage, interstitial oedema and thickening of the alveolar septum were observed by hematoxylin and eosin staining. (B) The degree of lung tissues injury was evaluated by lung injury score. ***P<0.001 vs. Sham; $^{\#\#}$P<0.01; and $^{\#\#\#}$P<0.001 vs. ALI. (C) The lung W/D ratio was examined. ***P<0.001 vs. Sham; $^{\#\#\#}$P<0.001 vs. ALI. (D) The MPO activity in lung tissues was measured. ***P<0.001 vs. Sham; $^{\#\#\#}$P<0.001 vs. ALI. Except the lung W/D ratio, each experiment was performed in triplicate for each mouse (n=5 in each group). STG, structured triglyceride; LPS, lipopolysaccharide; ALI, acute lung injury; W/D, wet/dry weight; MPO, myeloperoxidase.

injected into LPS-induced ALI mice to verify whether STG regulates GPR120 in ALI. Following LPS administration, the lung tissues isolated from mice treated with STG exhibited markedly decreased neutrophil infiltration, haemorrhage, interstitial oedema and thickening of the alveolar septum (Fig. 3A). Moreover, STG could decrease the lung injury score in ALI mice (P<0.01; Fig. 3B). AH7614 reversed the inhibitory effect of STG on the degree of lung tissue injury (Fig. 3A). Additionally, AH7614 simultaneously weakened the lowering effect of STG on the lung injury score (P<0.01; Fig. 3B). As shown in Fig. 3C and D, STG treatment visibly decreased the lung W/D ratio (P<0.001) and MPO activity (P<0.001). Furthermore, AH7614 rescued the decreased lung W/D ratio and MPO activity caused by STG in the LPS-induced ALI mouse model (P<0.001).

STG attenuates lung inflammation and TAK1/NF-κB pathway activity in the LPS-induced ALI mouse model by enhancing GPR120. The GPR120 inhibitor, AH7614, was intravenously injected into ALI mice, and the expression levels of pro-inflammatory cytokines and the phosphorylation of p65 and TAK1 in lung tissues were assessed. As displayed in Fig. 4A, the expression levels of IL-1β, IL-6 and TNF-α in lung tissues in the ALI + STG group were lower compared with those in the ALI group (P<0.001). Interestingly, AH7614 treatment clearly mitigated the suppressive effects of STG on the expression levels of IL-1β, IL-6 and TNF-α in lung tissues in the LPS-induced ALI mouse model (P<0.01). p65 is a major subunit of NF-κB. The p-TAK1/TAK1 and p-p65/p65 ratios were used to evaluate the activity of the TAK1/NF-κB pathway. The p-TAK1/TAK1 and p-p65/p65 ratios were clearly decreased by STG treatment, and AH7614 reversed the inhibitory effects of STG on the p-TAK1/TAK1 and p-p65/p65 ratios in the LPS-induced ALI mouse model (P<0.001; Fig. 4B).

STG ameliorates lung inflammation and TAK1/NF-κB pathway activity in LPS-induced RAW264.7 cells by enhancing GPR120. To evaluate the effect of STG on ALI *in vitro*, LPS-induced RAW264.7 cells acted as the LPS-induced ALI model at the cellular level. As shown in Fig. 5A, treatment with STG-containing serum visibly decreased the expression levels of pro-inflammatory cytokines in LPS-induced RAW264.7 cells (P<0.001), and AH7614 reversed the inhibitory effects of STG on the expression levels of pro-inflammatory cytokines (P<0.001). Furthermore, treatment with STG-containing serum significantly repressed the TAK1/NF-κB pathway activity in LPS-induced RAW264.7 cells (P<0.001), and AH7614 rescued the suppressed TAK1/NF-κB pathway activity caused by STG-containing serum treatment (P<0.01; Fig. 5B). As displayed in Fig. 5C, the protein expression levels of TLR4 and NLRP3 in the LPS + STG serum group were lower compared with those in the LPS group (P<0.001), and AH7614 reversed the lowering effects of STG-containing serum treatment on the protein expression levels of TLR4 and NLRP3 in LPS-induced RAW264.7 cells (P<0.05).

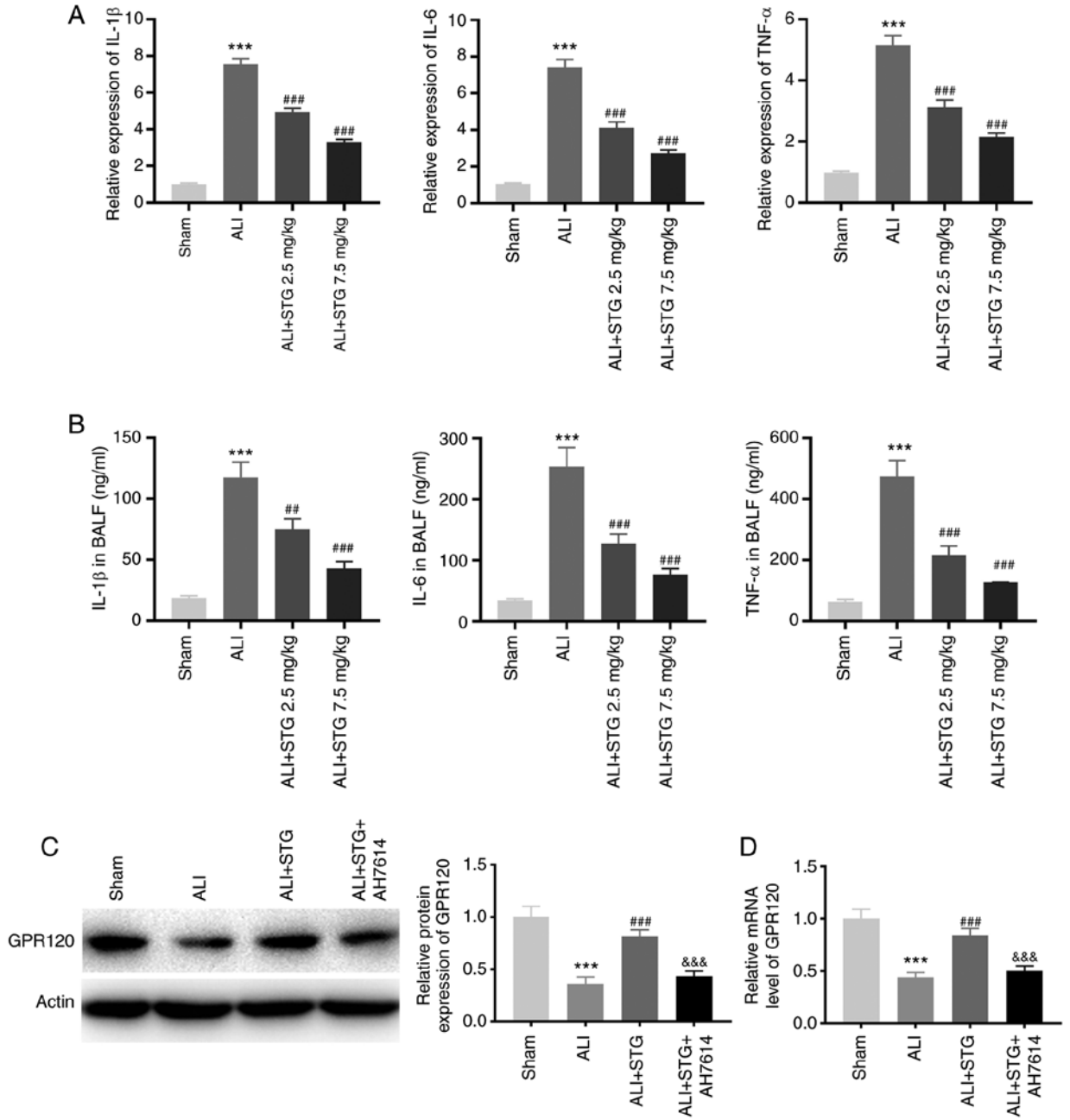

Figure 2. STG attenuates lung inflammation in the LPS-induced ALI mouse model. (A) RT-qPCR was performed to confirm the expression of IL-1β, IL-6, and TNF-α in lung tissues. ***P<0.001 vs. Sham; ###P<0.001 vs. ALI. (B) The levels of IL-1β, IL-6 and TNF-α in BALF were measured by enzyme-linked immunosorbent assay. ***P<0.001 vs. Sham; ##P<0.01; and ###P<0.001 vs. ALI. (C) The GPR120 protein expression in lung tissues was detected by western blotting. ***P<0.001 vs. Sham; ###P<0.001 vs. ALI; &&&P<0.001 vs. ALI + STG; (D) RT-qPCR was performed to measure the GPR120 mRNA expression level in lung tissues. ***P<0.001 vs. Sham; ###P<0.001 vs. ALI; &&&P<0.001 vs. ALI + STG. Each experiment was performed in triplicate for each mouse (n=5 in each group). STG, structured triglyceride; LPS, lipopolysaccharide; ALI, acute lung injury; IL, interleukin; TNF-α, tumor necrosis factor-α; RT-qPCR, reverse transcription-quantitative PCR; BALF, bronchoalveolar lavage fluid.

Discussion

LPS facilitates the release of inflammatory cytokines and leads to lung injury, which is a well-known experimental model of ALI (22,23). In the present study, the lung pathological changes, lung W/D ratio, MPO activity, expression levels of pro-inflammatory cytokines and TAK1/NF-κB pathway activity were clearly increased in LPS-induced ALI mouse model. Previous studies have verified that the degree of lung injury and inflammatory response are both increased in LPS-induced ALI (24,25). All the aforementioned descriptions suggest that the LPS-induced ALI mouse model was established successfully.

In the present study, STG decreased the lung pathological changes, lung W/D ratio and MPO activity in the LPS-induced ALI mouse model. The functions of STG were similar to the previously described emulsions. For instance, perfluorocarbon emulsion decreases the lung W/D ratio and suppresses MPO activity in LPS-induced ALI (26). Pre-treatment with fish oil-based emulsion decreases macrophage infiltration and improves the lung endothelial barrier in intestinal ischaemia-reperfusion-induced ALI (27). Interestingly, STG

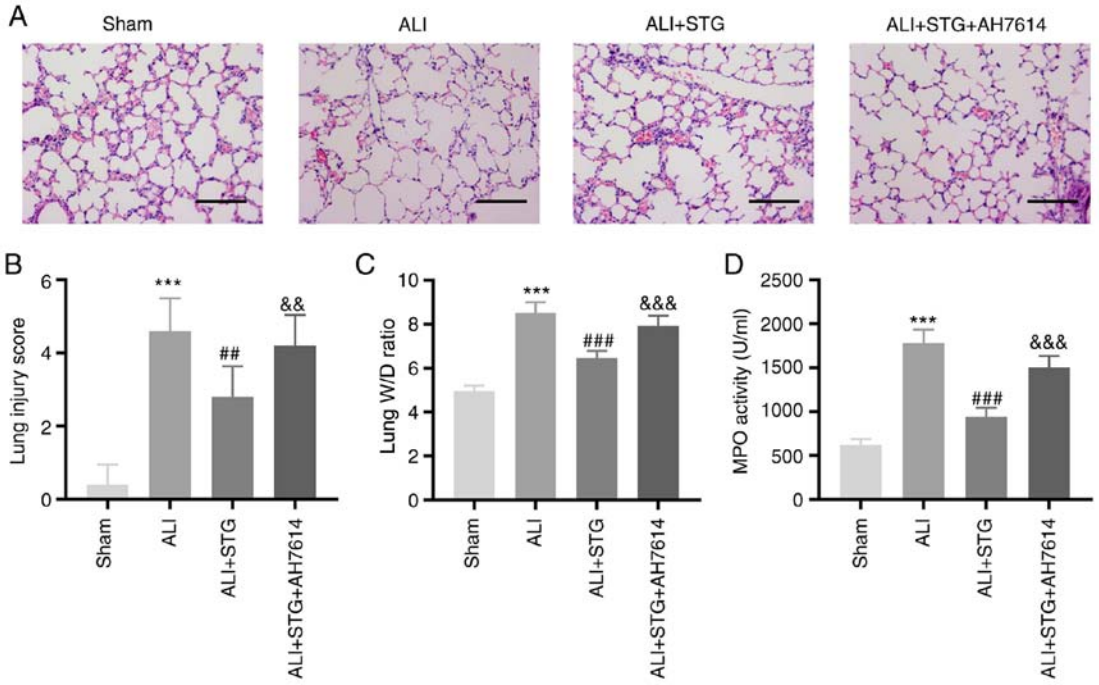

Figure 3. STG alleviates lung injury in the LPS-induced ALI mouse model by enhancing GPR120. (A) Hematoxylin and eosin staining was performed to assess the lung pathological changes, such as neutrophil infiltration, haemorrhage, interstitial oedema and thickening of the alveolar septum. (B) The degree of lung tissues injury was evaluated by lung injury score. ***P<0.001 vs. Sham; $^{\#\#}$P<0.01 vs. ALI; $^{\&\&}$P<0.01 vs. ALI + STG. (C) The lung W/D ratio was calculated. ***P<0.001 vs. Sham; $^{\#\#\#}$P<0.001 vs. ALI; $^{\&\&\&}$P<0.001 vs. ALI + STG. (D) The MPO activity in lung tissues was measured. ***P<0.001 vs. Sham; $^{\#\#\#}$P<0.001 vs. ALI; $^{\&\&\&}$P<0.001 vs. ALI + STG. Except the lung W/D ratio, each experiment was performed in triplicate for each mouse (n=5 in each group). STG, structured triglyceride; LPS, lipopolysaccharide; ALI, acute lung injury; W/D, wet/dry weight; MPO, myeloperoxidase.

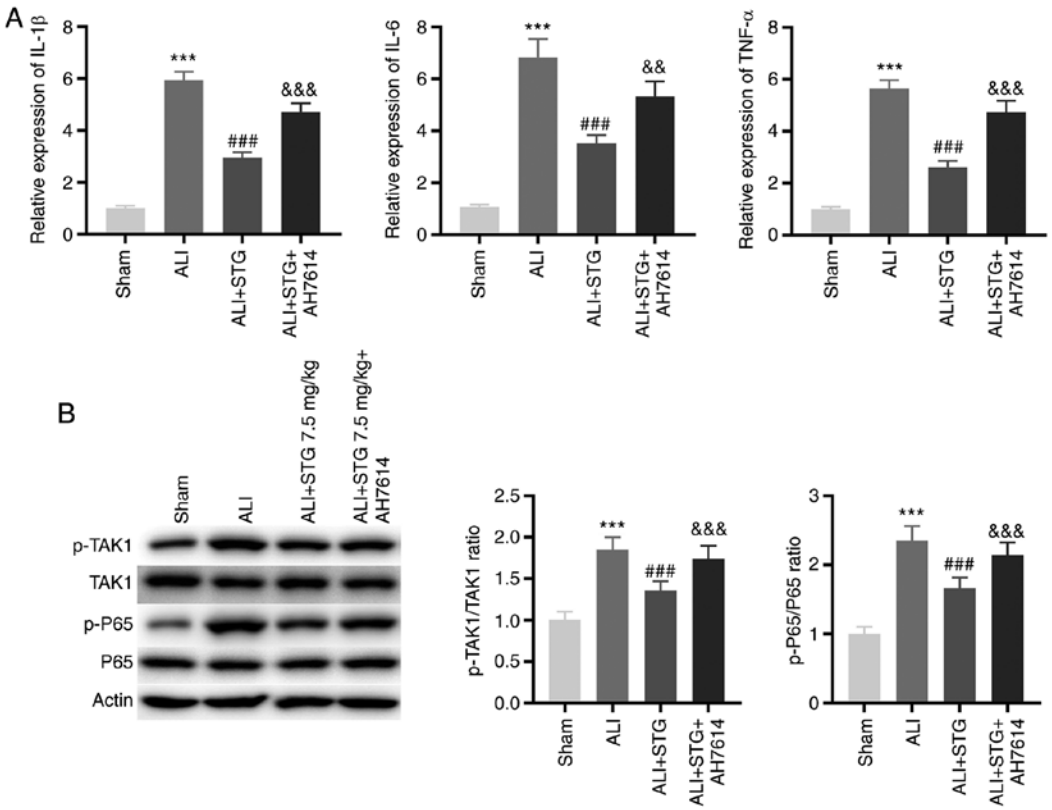

Figure 4. STG attenuates lung inflammation and TAK1/nuclear factor-κB pathway activity in the LPS-induced ALI mouse model by enhancing GPR120. (A) The expression of IL-1β, IL-6 and TNF-α in lung tissues was detected by reverse transcription-quantitative PCR. ***P<0.001 vs. Sham; $^{\#\#\#}$P<0.001 vs. ALI, $^{\&\&}$P<0.01; and $^{\&\&\&}$P<0.001 vs. ALI + STG. (B) Western blotting was performed to assess the activity of TAK1 and NF-κB pathway in lung tissues. ***P<0.001 vs. Sham; $^{\#\#\#}$P<0.001 vs. ALI; $^{\&\&\&}$P<0.001 vs. ALI + STG. Each experiment was performed in triplicate for each mouse (n=5 in each group). STG, structured triglyceride; LPS, lipopolysaccharide; ALI, acute lung injury; TAK, transforming growth factor-α-activated kinase; IL, interleukin; TNF-α, tumor necrosis factor-α; p-, phosphorylated.

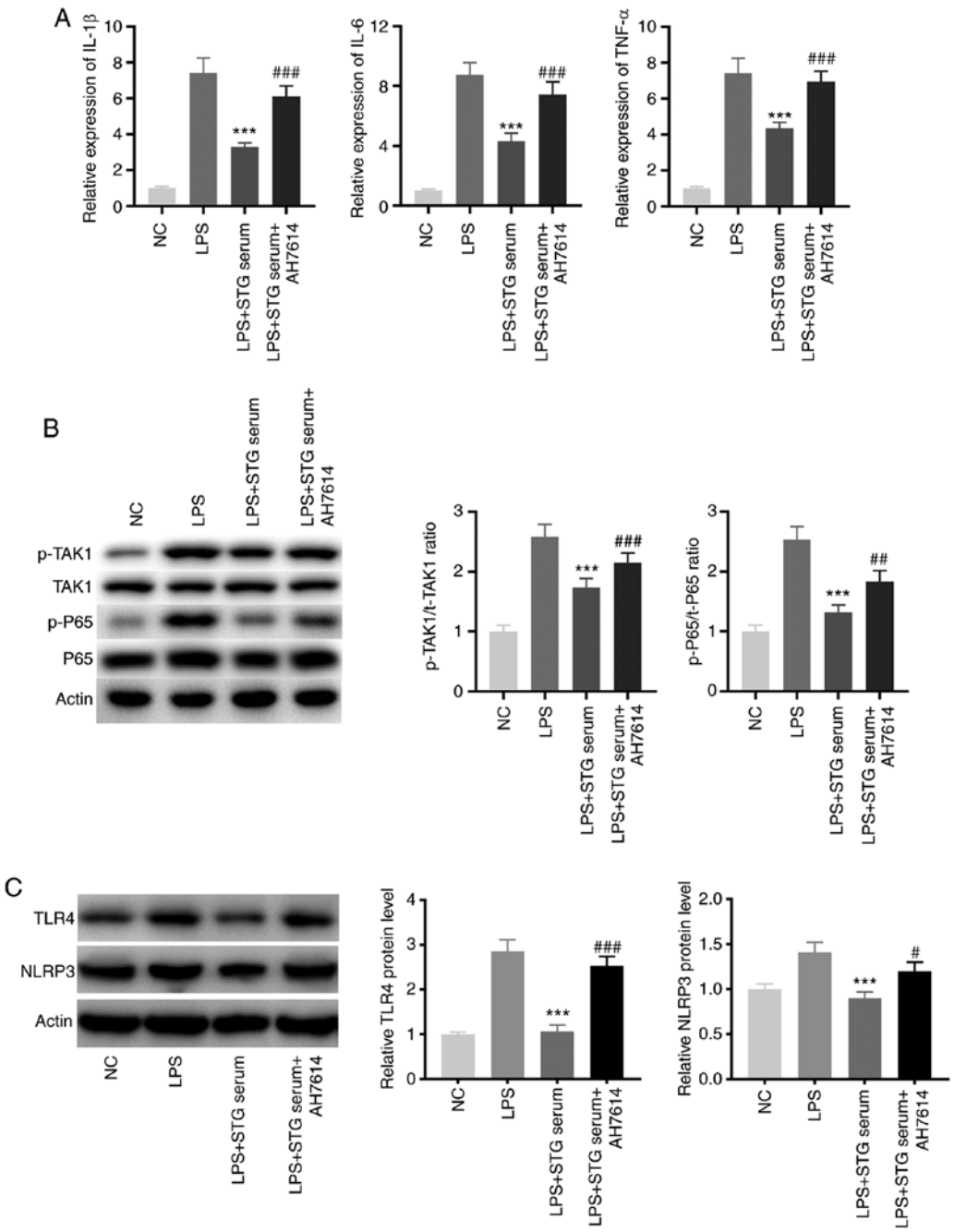

Figure 5. STG ameliorates lung inflammation and TAK1/nuclear factor-κB pathway activity in LPS-induced RAW264.7 cells by enhancing GPR120. (A) The levels of IL-1β, IL-6 and TNF-α in LPS-induced RAW264.7 cells were measured by reverse transcription-quantitative PCR. ***P<0.001 vs. LPS; $^{###}$P<0.001 vs. LPS + STG serum. (B) The activity of TAK1 and NF-κB pathway was evaluated by western blotting. ***P<0.001 vs. LPS; $^{##}$P<0.01 and $^{###}$P<0.001 vs. LPS + STG serum. (C) Western blotting was performed to measure the protein expression of TLR4 and NLRP3. ***P<0.001 vs. LPS; $^{#}$P<0.05 and $^{###}$P<0.001 vs. LPS + STG serum. Each experiment was performed in triplicate and repeated three times. STG, structured triglyceride; LPS, lipopolysaccharide; ALI, acute lung injury; NC, negative control; TAK, transforming growth factor-α-activated kinase; IL, interleukin, TNF-α, tumor necrosis factor-α; p-, phosphorylated; TLR, Toll-like receptor; NLRP3, family pyrin domain-containing 3.

retains the hepatic integrity in patients undergoing abdominal surgery (28). Among these options, it is suggested that treatment with STG may attenuate lung injury in ALI. Some lipids exert protective functions in different diseases by alleviating inflammation. For example, certain dietary oils (borage oil or fish oil) suppress pulmonary inflammation in patients with acute respiratory distress syndrome (29). Fish oil-based lipid emulsion decreases the generation of pro-inflammatory cytokines in LPS-induced ALI (30). Importantly, STG represses the expression levels of TNF-α, IL-6 and IFN-γ in the renal tissue of diabetic rats (13). In the present study, STG decreased the expression levels of pro-inflammatory cytokines in the LPS-induced ALI mouse model, indicating that STG hampers lung inflammation in ALI. To further verify the regulation of inflammation by STG in ALI, LPS-induced RAW264.7 cells were utilised. STG attenuated the inflammation in LPS-induced RAW264.7 cells. In summary, STG may protect against ALI by suppressing lung injury and inflammation. Nowadays, the roles of STG have been identified in different patients, such as moderately catabolic patients (31),

as well as those receiving liver resection (32), and parenteral nutrition (33). However, the anti-inflammatory effect of STG on lung injury in humans remains unclear. In addition, the advantages of this drug in comparison with other conventional drugs have not been determined. Further research on these topics is still needed.

It has been documented that the protein expression of certain GPRs is inhibited in different diseases, such as GPR40 in ureteral obstructed kidneys (34), GPR55 in Crohn's disease (35) and GPR120 in osteoarthritis (36). Similarly, GPR120 protein expression was decreased in the LPS-induced ALI mouse model in the present study. The GPR family exerts protective functions in various lung diseases. For instance, activation of GPR kinase (GRK)-2 decreases the lung injury score, MPO activity and lung inflammation in endotoxin-induced ALI (37). GRK-6 deficiency increases lung pathological changes and inflammatory cytokine expression levels in an *Escherichia coli* lung infection mouse model (38). Importantly, GPR120 has protective effects against different diseases. GPR120 alleviates acute kidney injury by suppressing apoptosis and ER stress (39). In addition, GPR120 mediates anti-inflammatory actions in immortalised hypothalamic neurons (40). Here, STG enhanced GPR120 protein expression in the LPS-induced ALI mouse model. Above all, it was suggested that STG protects against LPS-induced ALI by enhancing GPR120 expression. Encouragingly, feedback experiments demonstrated that AH7614 reversed the lowering effects of STG on the pathological changes in the lung, lung W/D ratio, MPO activity and lung inflammation in the LPS-induced ALI mouse model. *In vitro*, AH7614 reversed the suppressive effect of STG on inflammation in LPS-induced RAW264.7 cells. Taken together, these results suggest that STG alleviates the lung injury and inflammation in ALI by enhancing GPR120 expression.

TAK1, a mitogen-activated protein kinase kinase kinase family member, has been characterised as a critical mediator in the inflammatory signalling pathway (41). Notably, NF-κB is the downstream signalling pathway of TAK1 (42), and their combination promotes the inflammatory response (43,44). In the present study, STG attenuated TAK1/NF-κB pathway activity in the LPS-induced ALI mouse model. Inhibition of TAK1/NF-κB pathway activity has a suppressive effect on different diseases. For instance, tubulointerstitial inflammation is ameliorated by TAK1/NF-κB pathway suppression in proteinuric kidney disease (45) and inhibition of the TAK1/NF-κB pathway attenuates LPS-induced ALI (46). Thus, STG may protect against LPS-induced ALI by limiting the TAK1/NF-κB pathway. Previous studies have confirmed that there is a negative association between GPR120 and the TAK1 pathway, as well as between GPR120 and the NF-κB pathway. For example, GPR120 specifically decreases TAK1 phosphorylation and activation in human embryonic kidney 293 cells (47). GPR120 protects the liver from hepatic ischaemia-reperfusion injury by attenuating the NF-κB-mediated inflammatory response (48). Notably, GPR120 protein expression is decreased and TAK1/NF-κB protein expression is increased in bladder inflammation (49). In the present study, considering the interaction between STG and GPR120, it was assumed that STG may inhibit TAK1/NF-κB pathway activity by enhancing GPR120 expression in ALI. Interestingly, feedback experiments displayed that AH7614 weakened the inhibitory effect of STG on TAK1/NF-κB pathway activity in the LPS-induced ALI mouse model. The effect of STG on TAK1/NF-κB pathway activity was further evaluated *in vitro*. STG not only decreased the p-TAK1/TAK1 and p-p65/p65 ratios but also inhibited the protein expression levels of TLR4 (an upstream target of TAK1) (50,51) and NLRP3 (a downstream target of the NF-κB pathway) (52,53) in LPS-induced RAW264.7 cells, whereas AH7614 reversed the inhibitory effects exerted by STG. The present results suggest that the GPR120-TAK1/NF-κB pathway axis participated in the regulation of ALI. In summary, STG may attenuate TAK1/NF-κB pathway activity by enhancing GPR120 expression, thereby protecting against ALI.

In conclusion, a LPS-induced ALI mouse model was established to evaluate the regulatory effects of STG on lung injury and inflammation in ALI. The regulatory mechanism of STG associated with GPR120 and the TAK1/NF-κB pathway was further analysed. The present results show that STG may attenuate the lung injury and inflammation in ALI by regulating the GPR120-TAK1/NF-κB pathway axis. Thus, STG may be a valuable compound for treating ALI, and the GPR120-TAK1/NF-κB pathway axis may serve as a novel therapeutic target.

Acknowledgements

Not applicable.

Funding

The present study was supported by the project that Effect of structural triglycerides on early inflammatory response and respiratory function in patients with acute lung injury (grant no. 2017WSA17003).

Availability of data and materials

The datasets used and/or analyzed during the current study are available from the corresponding author on reasonable request.

Authors' contributions

Conceptualization and performing the experiments: HS and YP. Formal analysis and investigation: WL. Writing-original draft preparation: HS. Writing-review and editing: DZ. Funding acquisition: HS and WL. Resources: YP and DZ. Supervision: WL. Data analysis and interpretation: HS, DZ and WL. All authors read and approved the final manuscript.

Ethics approval and consent to participate

The animal experiments were permitted by the Ethics Committee of Heze Municipal Hospital (approval no. KYLL-hzsl2020008).

Patient consent for publication

Not applicable.

Competing interests

The authors declare that they have no competing interests.

References

1. Bhargava M and Wendt CH: Biomarkers in acute lung injury. Transl Res 159: 205-217, 2012.
2. Butt Y, Kurdowska AK and Allen TC: Acute lung injury: A clinical and molecular review. Arch Pathol Lab Med 140: 345-350, 2016.
3. Elicker BM, Jones KT, Naeger DM and Frank JA: Imaging of acute lung injury. Radiol Clin North Am 54: 1119-1132, 2016.
4. Mowery NT, Terzian WTH and Nelson AC: Acute lung injury. Curr Probl Surg 57: 100777, 2020.
5. Janz DR and Ware LB: Biomarkers of ALI/ARDS: Pathogenesis, discovery, and relevance to clinical trials. Semin Respir Crit Care Med 34: 537-548, 2013.
6. Lekka ME, Liokatis S, Nathanail C, Galani V and Nakos G: The impact of IV fat emulsion administration in acute lung injury. Nutr Clin Pract 19: 531-532, 2004.
7. Shih JM, Shih YM, Pai MH, Hou YC, Yeh CL and Yeh SL: Fish oil-based fat emulsion reduces acute kidney injury and inflammatory response in antibiotic-treated polymicrobial septic mice. Nutrients 8: 165, 2016.
8. Schaefer MB, Ott J, Mohr A, Bi MH, Grosz A, Weissmann N, Ishii S, Grimminger F, Seeger W and Mayer K: Immunomodulation by n-3-versus n-6-rich lipid emulsions in murine acute lung injury-role of platelet-activating factor receptor. Crit Care Med 35: 544-554, 2007.
9. Lekka ME, Liokatis S, Nathanail C, Galani V and Nakos G: The impact of intravenous fat emulsion administration in acute lung injury. Am J Respir Crit Care Med 169: 638-644, 2004.
10. Ishitsuka Y, Moriuchi H, Yang C, Golbidi S, Irikura M and Irie T: Effects of bolus injection of soybean-based fat emulsion and fatty acids on pulmonary gas exchange function. Biol Pharm Bull 32: 500-503, 2009.
11. Wu GH, Zaniolo O, Schuster H, Schlotzer E and Pradelli L: Structured triglycerides versus physical mixtures of medium- and long-chain triglycerides for parenteral nutrition in surgical or critically ill adult patients: Systematic review and meta-analysis. Clin Nutr 36: 150-161, 2017.
12. Lin M, Yeh SL, Tsou SS, Wang MY and Chen WJ: Effects of parenteral structured lipid emulsion on modulating the inflammatory response in rats undergoing a total gastrectomy. Nutrition 25: 115-121, 2009.
13. Das K and Ghosh M: Structured DAG oil ameliorates renal injury in streptozotocin-induced diabetic rats through inhibition of NF-κB and activation of Nrf2 pathway. Food Chem Toxicol 100: 225-238, 2017.
14. Marinissen MJ and Gutkind JS: G-protein-coupled receptors and signaling networks: Emerging paradigms. Trends Pharmacol Sci 22: 368-376, 2001.
15. Ren Z, Chen L, Wang Y, Wei X, Zeng S, Zheng Y, Gao C and Liu H: Activation of the omega-3 fatty acid receptor GPR120 protects against focal cerebral ischemic injury by preventing inflammation and apoptosis in mice. J Immunol 202: 747-759, 2019.
16. Gaspar RC, Veiga CB, Bessi MP, Dátilo MN, Sant'Ana MR, Rodrigues PB, de Moura LP, da Silva ASR, Santos GA, Catharino RR, *et al*: Unsaturated fatty acids from flaxseed oil and exercise modulate GPR120 but not GPR40 in the liver of obese mice: A new anti-inflammatory approach. J Nutr Biochem 66: 52-62, 2019.
17. Wanten GJ and Calder PC: Immune modulation by parenteral lipid emulsions. Am J Clin Nutr 85: 1171-1184, 2007.
18. Oh DY, Talukdar S, Bae EJ, Imamura T, Morinaga H, Fan W, Li P, Lu WJ, Watkins SM and Olefsky JM: GPR120 is an omega-3 fatty acid receptor mediating potent anti-inflammatory and insulin-sensitizing effects. Cell 142: 687-698, 2010.
19. Huang Q, Wang T and Wang HY: Ginsenoside Rb2 enhances the anti-inflammatory effect of ω-3 fatty acid in LPS-stimulated RAW264.7 macrophages by upregulating GPR120 expression. Acta Pharmacol Sin 38: 192-200, 2017.
20. Wang Y, Xu CF, Liu YJ, Mao YF, Lv Z, Li SY, Zhu XY and Jiang L: Salidroside attenuates ventilation induced lung injury via SIRT1-dependent inhibition of NLRP3 inflammasome. Cell Physiol Biochem 42: 34-43, 2017.
21. Livak KJ and Schmittgen TD: Analysis of relative gene expression data using real-time quantitative PCR and the 2(-Delta Delta C(T)) method. Methods 25: 402-408, 2001.
22. Lv H, Liu Q, Wen Z, Feng H, Deng X and Ci X: Xanthohumol ameliorates lipopolysaccharide (LPS)-induced acute lung injury via induction of AMPK/GSK3β-Nrf2 signal axis. Redox Biol 12: 311-324, 2017.
23. Zhu T, Wang DX, Zhang W, Liao XQ, Guan X, Bo H, Sun JY, Huang NW, He J, Zhang YK, *et al*: Andrographolide protects against LPS-induced acute lung injury by inactivation of NF-κB. PLoS One 8: e56407, 2013.
24. Lei J, Wei Y, Song P, Li Y, Zhang T, Feng Q and Xu G: Cordycepin inhibits LPS-induced acute lung injury by inhibiting inflammation and oxidative stress. Eur J Pharmacol 818: 110-114, 2018.
25. Zhang HX, Liu SJ, Tang XL, Duan GL, Ni X, Zhu XY, Liu YJ and Wang CN: H2S attenuates LPS-induced acute lung injury by reducing oxidative/nitrative stress and inflammation. Cell Physiol Biochem 40: 1603-1612, 2016.
26. Hou S, Ding H, Lv Q, Yin X, Song J, Landén NX and Fan H: Therapeutic effect of intravenous infusion of perfluorocarbon emulsion on LPS-induced acute lung injury in rats. PLoS One 9: e87826, 2014.
27. Jing H, Yao J, Liu X, Fan H, Zhang F, Li Z, Tian X and Zhou Y: Fish-oil emulsion (omega-3 polyunsaturated fatty acids) attenuates acute lung injury induced by intestinal ischemia-reperfusion through adenosine 5'-monophosphate-activated protein kinase-sirtuin1 pathway. J Surg Res 187: 252-261, 2014.
28. Piper SN, Röhm KD, Boldt J, Odermatt B, Maleck WH and Suttner SW: Hepatocellular integrity in patients requiring parenteral nutrition: Comparison of structured MCT/LCT vs a standard MCT/LCT emulsion and a LCT emulsion. Eur J Anaesthesiol 25: 557-565, 2008.
29. Mizock BA and DeMichele SJ: The acute respiratory distress syndrome: Role of nutritional modulation of inflammation through dietary lipids. Nutr Clin Pract 19: 563-574, 2004.
30. Hecker M, Linder T, Ott J, Walmrath HD, Lohmeyer J, Vadász I, Marsh LM, Herold S, Reichert M, Buchbinder A, *et al*: Immunomodulation by lipid emulsions in pulmonary inflammation: A randomized controlled trial. Crit Care 19: 226, 2015.
31. Zhao Y and Wang C: Meta-analysis of structured triglyceride versus physical mixture medium- and long-chain triglycerides for PN in liver resection patients. Biomed Res Int 2017: 4920134, 2017.
32. Kruimel JW, Naber TH, van der Vliet JA, Carneheim C, Katan MB and Jansen JB: Parenteral structured triglyceride emulsion improves nitrogen balance and is cleared faster from the blood in moderately catabolic patients. JPEN J Parenter Enteral Nutr 25: 237-244, 2001.
33. Li C, Ni Q, Pei Y, Ren Y and Feng Y: Meta-analysis of the efficacy and safety of structured triglyceride lipid emulsions in parenteral nutrition therapy in China. Clin Nutr 38: 1524-1535, 2019.
34. Kim CS, Joo SY, Kim IJ, Choi HI, Bae EH, Kim SW and Ma SK: Anti-apoptotic effect of G-protein-coupled receptor 40 activation on tumor necrosis factor-α-induced injury of rat proximal tubular cells. Int J Mol Sci 20: 3386, 2019.
35. Wlodarczyk M, Sobolewska-Włodarczyk A, Cygankiewicz AI, Jacenik D, Krajewska WM, Stec-Michalska K, Piechota-Polańczyk A, Wiśniewska-Jarosińska M and Fichna J: G protein-coupled receptor 55 (GPR55) expresses differently in patients with Crohn's disease and ulcerative colitis. Scand J Gastroenterol 52: 711-715, 2017.
36. Lu M and Zhou E: Long noncoding RNA LINC00662-miR-15b-5p mediated GPR120 dysregulation contributes to osteoarthritis. Pathol Int 70: 155-165, 2020.
37. Su VY, Chiou SH, Lin CS, Chen WC, Yu WK, Chen YW, Chen CY and Yang KY: Induced pluripotent stem cells reduce neutrophil chemotaxis via activating GRK2 in endotoxin-induced acute lung injury. Respirology 22: 1156-1164, 2017.
38. Lee T, Packiriswamy N, Lee E, Lucas PC, Mccabe LR and Parameswaran N: Role of G protein-coupled receptor kinase-6 in *Escherichia coli* lung infection model in mice. Physiol Genomics 49: 682-689, 2017.
39. Huang Z, Guo F, Xia Z, Liang Y, Lei S, Tan Z, Ma L and Fu P: Activation of GPR120 by TUG891 ameliorated cisplatin-induced acute kidney injury via repressing ER stress and apoptosis. Biomed Pharmacother 126: 110056, 2020.
40. Wellhauser L and Belsham DD: Activation of the omega-3 fatty acid receptor GPR120 mediates anti-inflammatory actions in immortalized hypothalamic neurons. J Neuroinflammation 11: 60, 2014.

41. Sakurai H: Targeting of TAK1 in inflammatory disorders and cancer. Trends Pharmacol Sci 33: 522-530, 2012.
42. Gao D, Wang R, Li B, Yang Y, Zhai Z and Chen DY: WDR34 is a novel TAK1-associated suppressor of the IL-1R/TLR3/TLR4-induced NF-kappaB activation pathway. Cell Mol Life Sci 66: 2573-2584, 2009.
43. Wang W, Xia T and Yu X: Wogonin suppresses inflammatory response and maintains intestinal barrier function via TLR4-MyD88-TAK1-mediated NF-κB pathway in vitro. Inflamm Res 64: 423-431, 2015.
44. Wang Y, Tu Q, Yan W, Xiao D, Zeng Z, Ouyang Y, Huang L, Cai J, Zeng X, Chen YJ and Liu A: CXC195 suppresses proliferation and inflammatory response in LPS-induced human hepatocellular carcinoma cells via regulating TLR4-MyD88-TAK1-mediated NF-κB and MAPK pathway. Biochem Biophys Res Commun 456: 373-379, 2015.
45. Yang X, Kume S, Tanaka Y, Isshiki K, Araki S, Chin-Kanasaki M, Sugimoto T, Koya D, Haneda M, Sugaya T, *et al*: GW501516, a PPARδ agonist, ameliorates tubulointerstitial inflammation in proteinuric kidney disease via inhibition of TAK1-NFκB pathway in mice. PLoS One 6: e25271, 2011.
46. Yang S, Yu Z, Yuan T, Wang L, Wang X, Yang H, Sun L, Wang Y and Du G: Therapeutic effect of methyl salicylate 2-O-β-d-lactoside on LPS-induced acute lung injury by inhibiting TAK1/NF-kappaB phosphorylation and NLRP3 expression. Int Immunopharmacol 40: 219-228, 2016.
47. Hara T, Hirasawa A, Ichimura A, Kimura I and Tsujimoto G: Free fatty acid receptors FFAR1 and GPR120 as novel therapeutic targets for metabolic disorders. J Pharm Sci 100: 3594-3601, 2011.
48. Baker MA, Nandivada P, Mitchell PD, Fell GL, Pan A, Cho BS, De La Flor DJ, Anez-Bustillos L, Dao DT, Nosé V and Puder M: Omega-3 fatty acids are protective in hepatic ischemia reperfusion injury in the absence of GPR120 signaling. J Pediatr Surg 54: 2392-2397, 2019.
49. Chen YL, Lin YP, Sun CK, Huang TH, Yip HK and Chen YT: Extracorporeal shockwave against inflammation mediated by GPR120 receptor in cyclophosphamide-induced rat cystitis model. Mol Med 24: 60, 2018.
50. Meng Z, Si CY, Teng S, Yu XH and Li HY: Tanshinone IIA inhibits lipopolysaccharide-induced inflammatory responses through the TLR4/TAK1/NF-κB signaling pathway in vascular smooth muscle cells. Int J Mol Med 43: 1847-1858, 2019.
51. Sun P, Song SZ, Jiang S, Li X, Yao YL, Wu YL, Lian LH and Nan JX: Salidroside regulates inflammatory response in raw 264.7 macrophages via TLR4/TAK1 and ameliorates inflammation in alcohol binge drinking-induced liver injury. Molecules 21: 1490, 2016.
52. Yi H, Peng R, Zhang LY, Sun Y, Peng HM, Liu HD, Yu LJ, Li AL, Zhang YJ, Jiang WH and Zhang Z: LincRNA-Gm4419 knockdown ameliorates NF-κB/NLRP3 inflammasome-mediated inflammation in diabetic nephropathy. Cell Death Dis 8: e2583, 2017.
53. Bai Y, Li Z, Liu W, Gao D, Liu M and Zhang P: Biochanin A attenuates myocardial ischemia/reperfusion injury through the TLR4/NF-κB/NLRP3 signaling pathway. Acta Cir Bras 34: e201901104, 2019.